

SUPPORT INFORMATION

Eu and F co-doped ZnO-based transparent electrodes for organic and quantum dot light-emitting diodes

Jingsong Luo,^{a,b} Jie Lin,^{*a} Nan Zhang,^a Xiaoyang Guo,^a Ligong Zhang,^a Yongsheng Hu,^a
Ying Lv,^a Yongfu Zhu,^b and Xingyuan Liu^{*a}

^aState Key Laboratory of Luminescence and Applications, Changchun Institute of Optics,
Fine Mechanics and Physics, Chinese Academy of Sciences, Changchun 130033, China.

^bKey Laboratory of Automobile Materials, Ministry of Education, and School of
Materials Science and Engineering, Jilin University, Changchun 130022, China

Corresponding Authors

*E-mail: linj@ciomp.ac.cn, liuxy@ciomp.ac.cn.

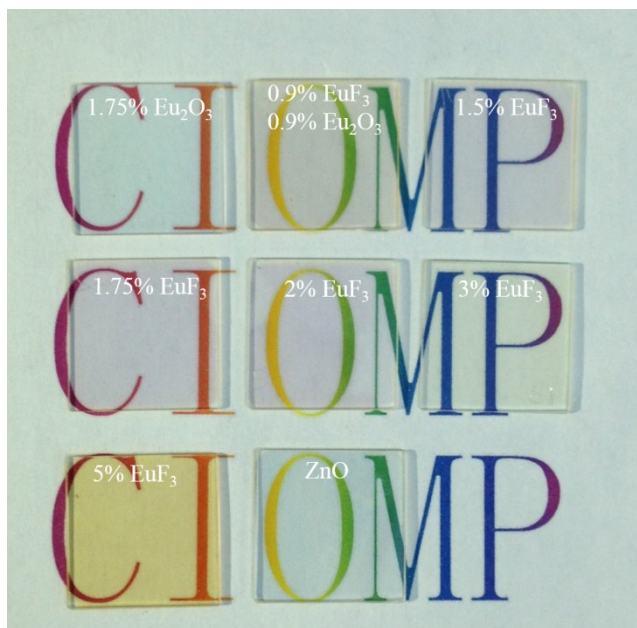


Figure S1. Pictures of EFZO samples with different Eu and F doping concentration.

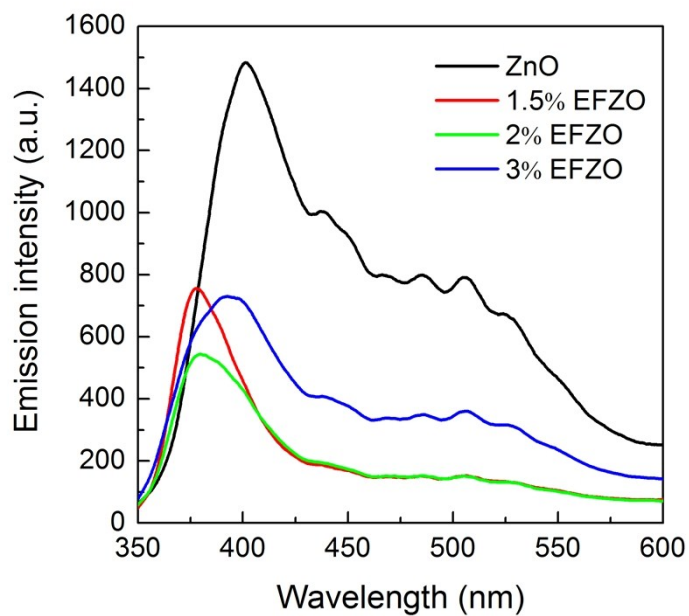


Figure S2. Photoluminescence spectra of the ZnO and EFZO samples.

The photoluminescence spectra of EFZO samples were measured with excitation

wavelength of 325 nm, which mainly shows emission characteristics of ZnO. Luminescence peaks centered around 380 nm and 500 nm presented in the spectra are attributed to the near band-edge (NBE) due to free excitonic emission ^[1-2], and are related to native point defects such as VO and VZn ^[3], respectively. F doping has been reported to first fill oxygen vacancy before replacing oxygen sites, because an oxygen vacancy has the lowest formation energy ^[4-5]. F doping has decreased concentration of oxygen vacancy, as an effective dopant and a defect-passivation agent, and thus has better crystallinity and increases carrier mobility, due to the substitutional doping of O ions with F ions and the filling of O-related defect sites ^[6]. Violet emission at 400 nm from undoped ZnO is not NBE transition (around 380 nm), which should derive from polycrystal of ZnO prepared by ion-assisted electron beam evaporation, different from single crystal of ZnO. These phenomena also happened in the work of Rotella et al. ^[3]. With the doping of EuF₃, corresponding to 1.5%, 2% and 3% EFZO samples, a clear blueshift is observed that represents the NBE transition. This transformation indicates that crystallinity has been improved significantly compared to undoped ZnO. A rational interpretation for blueshift is attributed to a band gap changing phenomenon by the higher carrier concentration through cation-doping in ZnO ^[5].

Simultaneously, a significant decrease in the intensity of the visible emission around 500 nm can result from a decrease in O vacancies, which indicates that F filling O vacancies leads to better crystallinity. However, compared with 1.5%, 2% doping, Eu and F excessively addition doping, 3%, the intensity of the visible emission increases slightly, but is lower than that of undoped ZnO, which shows the increase of VZn with Eu% that is in accordance with the work of Rotella et al.^[3]. Furthermore, according to Wang *et al*, VZn formation energy reduces with Al content ^[7], and the increased Zn vacancies concentration would result in the increase of the lattice parameter ^[3]. Similar to Al doping, Eu doping should have a similar effect. As showed in Fig. S2, spectral peaks around 500 nm for 1.5%, 2%, and 3% EFZO have decreased considerably in comparison with that of

ZnO. Nevertheless, peaks of 3% EFZO has increased relative to 1.5%, 2% EFZO. This shows that F doping has reduced oxygen vacancy indeed, but an excessive doping as in 3% EFZO has increased the Zn vacancy concentration. The lattice parameter should increase. However, the lattice parameter of 3% EFZO has decreased in comparison with that of 2% EFZO, and the mobility decreased dramatically yet.

The mobility decreases accompanied by a saturation of the charge carriers concentration [3]. Moreover, the mobility is mainly dominated by the ionized impurity scattering [8]. As a result, an increase of grain boundary density leads to the enhancement of scattering rate [2]. This has indicated that Eu and F codoping has a complementary effect to the reduction of lattice distortion. Thus we infer that Eu and F codoping should improve the properties of ZnO thin film, thereby suppressing the lattice deformation and increasing the mobility.

Finally, the small amount of Eu and F addition in ZnO acts as a point defect killer, and thus removes the in-grain scattering centers. However, heavily doping increases grain boundary scattering, causes a severe deterioration of crystallinity, and become the mobility limiting mechanism [9].

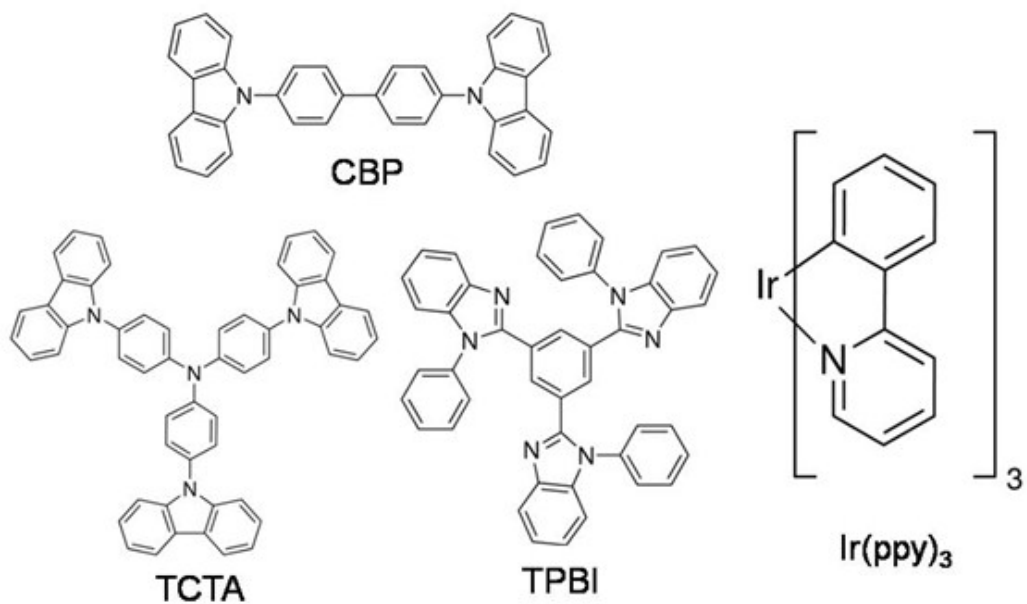


Figure S3. Molecular structure of the organic materials used in OLEDs.

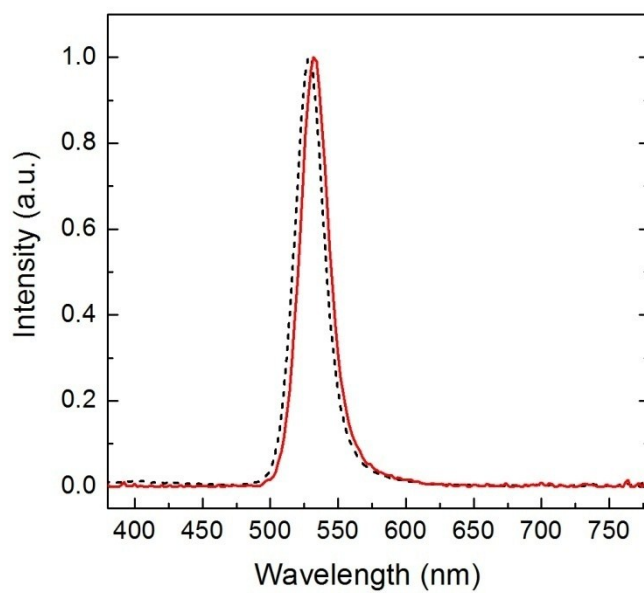


Figure S4. PL spectrum of QDs and EL spectrum of QLEDs in a broader spectrum scope.

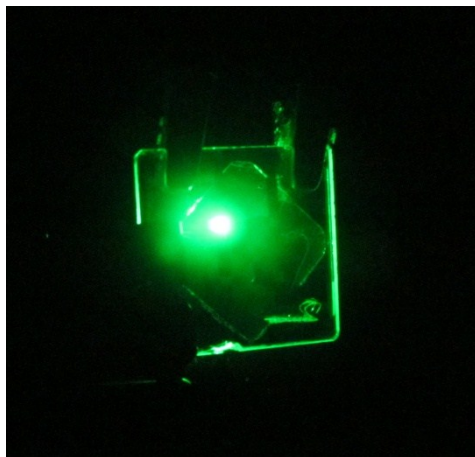


Figure S5. Photograph of the EFZO-based QLED.

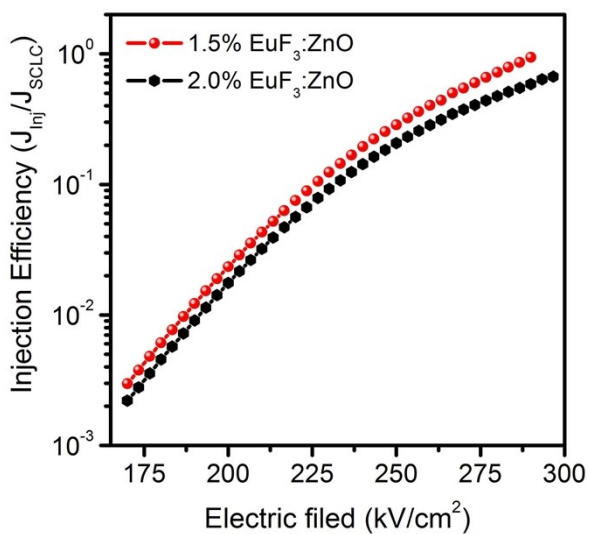


Figure S6. Hole injection efficiency (J_{INT}/J_{SCL}) of different electrodes as a function of electric field for the hole-only devices.

Hole injection efficiency was calculated by $\eta_{INJ}=J_{INJ}/J_{SCL}$, where J_{INJ} and J_{SCL} are the measured current density and the calculated theoretical value of the space-charge-limited current (SCLC). The two hole injection devices have the following structures:

1.5 % EuF₃ device: 1.5 % EuF₃ : ZnO/TCTA (100 nm)/LiF (1 nm) /Al;

2.0 % EuF₃ device: 2.0 % EuF₃: ZnO /TCTA (100 nm) /LiF (1 nm)/Al.

The results show that 1.5% EuF₃ doped ZnO film has a higher hole injection efficiency than 2.0% EuF₃ doped ZnO film, and is better to serve as an anode for OLEDs.

Table S1. The electrical parameters of EFZO films with varying dopant contents

| Eu/F: ZnO sample | Resistivity [$\Omega \cdot \text{cm}$] | Carrier density [cm^{-3}] | Mobility [$\text{cm}^2/\text{V} \cdot \text{s}$] | Work function [eV] |
|--|---|---|---|-----------------------|
| 1.75% Eu ₂ O ₃ | 9.08E-03 | -3.04E+19 | 22.6 | 4.97 |
| 0.9% EuF ₃ 0.9% Eu ₂ O ₃ | 1.43E-03 | -1.34E+20 | 32.5 | 4.88 |
| 1.5% EuF ₃ | 6.15E-04 | -1.76E+20 | 57.8 | 4.92 |
| 1.75% EuF ₃ | 5.70E-04 | -1.86E+20 | 58.8 | 4.9 |
| 2% EuF ₃ | 5.57E-04 | -1.93E+20 | 58.1 | 4.88 |
| 3% EuF ₃ | 9.41E-04 | -1.58E+20 | 42.1 | 4.89 |
| 5% EuF ₃ | 3.01E-03 | -9.47E+19 | 21.9 | 4.97 |
| ZnO | 4.08E-02 | -3.74E+18 | 40.9 | 4.9 |

Table S2. Comparison of EL characteristics of OLEDs

| Device | Anode | V _{on} [V] | L _{max} [cd/m^2] | CE _{max} [cd/A] | EQE _{max} [%] | LE _{max} [lm/w] |
|--------|-------|------------------------|--|---|---------------------------|---|
| OLED | EFZO | 2.47 | 103000 | 60.3 | 20.9 | 76.65 |
| OLED | ITO | 3.09 | 112000 | 54.76 | 19.8 | 55.68 |

V_{on}: turn-on voltage, obtained at a luminance of 1 cd/m^2 ; L_{max}: maximum luminance; CE_{max}: maximum current efficiency; LE_{max}: maximum luminous efficiency; EQE_{max}: maximum external quantum efficiency.

Table S3. Comparison of EL characteristics of QLEDs

| Device | Cathode | V _{on} [V] | L _{max} [cd/m ²] | CE _{max} [cd/A] | EQE _{max} [%] | LE _{max} [lm/w] |
|--------|---------|------------------------|--|-----------------------------|---------------------------|-----------------------------|
| QLED | EFZO | 3.66 | 128000 | 21.6 | 4.21 | 8.97 |
| QLED | ITO | 3.48 | 117000 | 18.2 | 4.25 | 8.41 |

V_{on}: turn-on voltage, obtained at a luminance of 1 cd/m²; L_{max}: maximum luminance; CE_{max}: maximum current efficiency; LE_{max}: maximum luminous efficiency; EQE_{max}: maximum external quantum efficiency.

Table S4. The electrical and optical properties of ITO used in the reference device

| | Resistivity [Ω·cm] | Carrier density [cm ⁻³] | Mobility [cm ² /V·s] | Work function [eV] | Average transmittance (400-700 nm) [%] | Film Thickness [nm] |
|-----|-----------------------|---|------------------------------------|--------------------------|---|---------------------------|
| ITO | 3.9E-04 | 6.1E+20 | 26.8 | 4.65 | 86.5 | 120 |

References

- [1] J. Alloy. Compd. 2015, **646**, 56-62.
- [2] J. Phys. Chem. C 2017, **121**, 16012–16020.
- [3] J. Phys. D: Appl. Phys. 2017, **50**, 485106.
- [4] Appl. Phys. Lett. 2010, **97**, 122101.
- [5] Sol. Energ. Mat. Sol. C. 2015, **132**, 403-409.
- [6] J. Mater. Chem. C, 2014, **2**, 98-108.
- [7] Appl. Phys. Lett. 2012, **100**, 132407.
- [8] Thin Solid Films 2000, **366**, 63-68.
- [9] J. Appl. Phys. 2006, **100**, 063701.

